# Project Number 282910

# ÉCLAIRE

# Effects of Climate Change on Air Pollution Impacts and Response Strategies for European Ecosystems

**Seventh Framework Programme**

**Theme: Environment**

# D3.2. Background bi-directional NH3 exchange with soil/vegetation module

Due date of deliverable: **31/03/2014**

Actual submission date: **30/09/2015**

Start Date of Project: **01/10/2011**

Duration: **48 months**

Organisation name of lead contractor for this deliverable :
**Karlsruher Institut fuer Technologie**

| Project co-funded by the European Commission within the Seventh Framework Programme | | |
|---|---|---|
| **Dissemination Level** | | |
| **PU** | Public | ☐ |
| **PP** | Restricted to other programme participants (including the Commission Services) | ☒ |
| **RE** | Restricted to a group specified by the consortium (including the Commission Services) | ☐ |
| **CO** | Confidential, only for members of the consortium (including the Commission Services) | ☐ |

## 1. Executive Summary

- The objective of this task was to improve parameterisations and models of surface/atmosphere bi-directional $NH_3$ exchange with soil and vegetation for background conditions, i.e. for semi-natural ecosystems and for agro-ecosystems outside fertilisation events.
- The strategy to fulfill these requirements was to evaluate and refine an existing state-of-the-art parameterisation for bi-directional $NH_3$ exchange, the Massad-Nemitz-Sutton parameterisation scheme ("MNS-2010" hereafter; Massad et al., 2010).
- The stomatal emission potential ($\Gamma_s$) of semi-natural and agricultural vegetation was refined either by adjusting to existing datasets and the data generated within Eclaire for crops, grassland and forest, or by using crop modelling (CERES-EGC).
- CERES-EGC was also used to derive parameterisations of the soil emission potential ($\Gamma_g$) for background conditions (outside fertilisation events) for croplands across Europe. A meta-modelling approach was developed with the aim of deriving simplified empirical relationships between $\Gamma_g$ and management and environmental variables, which could then be implemented at low computational cost within chemical transport models (CTMs).
- The parameterisation of the non-stomatal resistance ($R_w$) to $NH_3$ deposition and its response to the pollution climate was adjusted to existing datasets and the data generated within Eclaire for crops, grassland and forest.
- The MNS-2010 model was evaluated against 3 datasets from unfertilised ecosystems (one moorland, one temperate mixed forest and one Mediterranean forest) and 5 datasets from fertilised ecosystems (three grazed grasslands, one cut grassland and one crop rotation) over Europe. An additional comparison was performed on a grassland site in Brittany.
- The $NH_3$ dry deposition fluxes using the default MNS-2010 scheme were systematically underestimated by comparison to measured flux values. A sensitivity analysis indicated that lowering $\Gamma_s$ values by a significant fraction would not significantly address the under-deposition issue in the model, but instead non-stomatal resistance to $NH_3$ deposition ($R_w$) was generally over-estimated and that its parameterisation should be revised. The proposed revision of the MNS-2010 consisted in dividing by 3 the minimum non-stomatal resistance and its response to temperature. This resulted in a significant improvement in model results and predictive capability when tested against ECLAIRE datasets.
- Soil and stomatal emission potential ($\Gamma_g$ and $\Gamma_s$) were obtained from runs of the CERES-EGC crop model for the whole of Europe on a daily time step and with a 0.25°×0.25° grid resolution for three periods: a historical period (1950-2010) and two future periods with two different scenarios RCP4.5 (2010-2100) and RCP8.5 (2010 – 2100).
- The soil data were extracted from the European soil database (Panagos et al., 2012) and were aggregated on the 0.25°×0.25° grid. Management data were extracted from the open access GHG-Europe project database and were initially provided by M. Wattenbach. The data contains the crop sequences from 1976 to 2010 on a 1 x 1 km grid which were aggregated in the 0.25°×0.25° grid. Meteorological data were derived from the HadGEM2-ES climate model for two scenarios as described above (RCP 4.5 and RCP 8.5).
- The $\Gamma_g$ ($\Gamma_s$) simulated with CERES-EGC for background conditions vary between 50 and 6000 (20 and 250) and lie within reported values in literature. The simulated stomatal emissions potentials were almost homogeneously distributed in Europe while soil emissions potentials are larger in alkaline soils. Maps of monthly $\Gamma_g$ and $\Gamma_s$ were produced on the 0.25°×0.25° grid
- A meta-model of yearly averaged $\Gamma_g$ was fitted to the simulated values which were shown to respond predominantly and positively to soil pH and fertilization rates and slightly but negatively to temperature and precipitation.
- Overall, an updated parameterisation of the MNS-2010 is proposed and a new methodology for deriving $\Gamma_g$ and $\Gamma_s$ is evaluated.

## 2. Objectives:

- The objective of WP 3.2 was to improve parameterisations and models of surface/atmosphere bi-directional $NH_3$ exchange with soil and vegetation for background conditions, i.e. for semi-natural ecosystems and for agro-ecosystems outside fertilisation events.
- New flux measurement data from the ECLAIRE flux network and from controlled soil and litter emission measurements within ECLAIRE, as well as flux data from earlier European projects (eg NitroEurope IP) and from parallel national activities, would be used both to test existing schemes and to develop or improve new model descriptions of background $NH_3$ exchange.
- Particular emphasis was to be given to the improvement of responses of $NH_3$ exchange to changes in meteorological conditions under a changing climate, such as temperature, leaf surface wetness and co-deposition of chemically interacting compounds.
- The strategy adopted to fulfil these requirements was twofold:
  1. To evaluate and refine an existing state-of-the-art parameterisation for bi-directional $NH_3$ exchange, the Massad-Nemitz-Sutton parameterisation scheme ("MNS-2010" hereafter; Massad et al., 2010), to address the stomatal emission potential ($\Gamma_s$) of semi-natural and agricultural vegetation, and the non-stomatal resistance ($R_w$) to $NH_3$ deposition and its response to the pollution climate.
  2. To use mechanistic crop modelling to derive parameterisations of the soil emission potential ($\Gamma_g$) for background conditions (outside fertilisation events) for croplands across Europe. More specifically, a meta-modelling approach was developed with the aim of deriving simplified empirical relationships between $\Gamma_g$ and management and environmental variables, which could then be implemented at low computational cost within chemical transport models (CTMs).

## 3. Activities:

*3.1 Evaluation and validation of the Massad-Nemitz-Sutton (2010) $NH_3$ exchange parameterisation for background conditions*

3.1.1 Basic description

The MNS-2010 parameterisation for bi-directional $NH_3$ exchange was based on an extensive literature review of $NH_3$ flux datasets, soil and vegetation emission potentials and resistance formulations for in-canopy transfer and deposition (Massad et al., 2010). The MNS-2010 scheme was developed to provide general parameter tables and functions for the Nemitz-Milford-Sutton 2-layer $NH_3$ canopy compensation point model ("NMS-2001" hereafter, Nemitz et al., 2001), with a view to implementing bi-directional $NH_3$ exchange schemes in CTMs. Briefly, the exchange of $NH_3$ between the atmosphere and the ecosystem is mediated by a network of physical resistances accounting for turbulent transfer above- and in-canopy, molecular diffusion through laminar sub-layers and through stomates, and uptake by wetness and by other non-stomatal surfaces (Fig. 1).

Unlike traditional dry deposition schemes still used in most CTMs (Wesely et al., 1989), compensation point models such as NMS-2001 allow for $NH_3$ emissions as well as deposition fluxes, based on the recognition that both plant leaves and the uppermost layers of topsoil and the leaf litter contain dissolved $NH_3$ and $NH_4^+$ (with a pH-dependent partitioning), which through Henry's law generate non-zero $NH_3$ gas surface potentials. The exchange is bi-directional because depending on ambient atmospheric $NH_3$ levels and other environmental factors (temperature, relative humidity, surface wetness), deposition to the ecosystem from the atmosphere may prevail over plant/soil emissions, or vice versa. The sign and magnitude of the net flux is controlled by the difference between air concentration ($\chi_a$) and the so-called canopy compensation point ($\chi_c$).

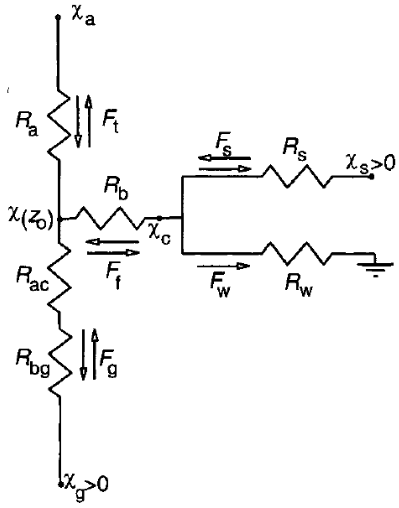


*Figure 1. The Nemitz-Milford-Sutton (NMS-2001) 2-layer canopy compensation point model.*

The key parameterisations examined and derived by Massad et al. (2010) focused on the stomatal compensation point ($\chi_s$), the soil surface $NH_3$ concentration ($\chi_g$) and the non-stomatal $R_w$. More specifically, since the solubility of $NH_3$ in water is temperature-dependent, a more useful (temperature-independent) measure of the $NH_3$ emission potential is the ammonium to proton ratio in the substrate, noted Γ hereafter. For example the Γ value for plant stomates is given as the ratio of concentrations in the apoplast:

$$\Gamma_s = \frac{[NH_4^+]_{apo}}{[H^+]_{apo}} \quad (1)$$

The ground/soil emission potential $\Gamma_g$ is given as:

$$\Gamma_g = \frac{[NH_4^+]_{soil}}{[H^+]_{soil}} \quad (2)$$

Major challenges in implementing Γ-based representations of plant and soil $NH_3$ emission potentials in CTMs include the need for Γ values for all ecosystem types across the modelling domain and their temporal variability over seasonal and multi-annual time scales (Flechard et al., 2013). Based on their review of published $\Gamma_s$ values, Massad et al. (2010) proposed that for unmanaged ecosystems $\Gamma_s$ should increase with atmospheric N deposition, or N input ($N_{IN}$), following:

$$\Gamma_s = 246 + 0.0041 * {N_{IN}}^{3.56} \qquad \text{(unmanaged)} \quad (3)$$

For managed (agricultural) systems during background periods they derived a similar form of relationship, in which $N_{IN}$ is the sum of annual fertilisation and atmospheric deposition:

$$\Gamma_s = 66.4 + 0.0853 * {N_{IN}}^{1.59} \qquad \text{(managed, background)} \quad (4)$$

Note that in this context, a "managed" ecosystem indicates either the occurrence of nitrogen fertilisation, or grazing by farm herbivores, or both. An unimproved grassland or moorland that is extensively grazed is referred to as managed even in the absence of mineral or organic N fertilisation. Figure 2 shows that for an identical N input level, the parameterised MNS-2010 value of $\Gamma_s$ is always higher for semi-natural vegetation than for agricultural systems (in the range of typical atmospheric N deposition 0-50 kgN $ha^{-1}$ $yr^{-1}$). In practice agro-ecosystems are typically fertilised with 100-200 kgN $ha^{-1}$ $yr^{-1}$, which yields typical background $\Gamma_s$ values of 200-400, thus very similar to unmanaged $\Gamma_s$ values for N deposition levels between 0 and 20 kgN $ha^{-1}$ $yr^{-1}$.

Note that the MNS-2010 scheme also provides parameterisations for short-term temporal changes in $\Gamma_s$ following the field application of mineral and organic fertilisers to agro-ecosystems, with the initial elevated $\Gamma_s$ value at the date/time of fertilisation being a linear function of the applied N fertiliser dose ($\Gamma_{s,max}$=12.3*$N_{app}$+20.3) and $\Gamma_s$ decreasing exponentially over the following few days ($\Gamma_s(t)=\Gamma_{s,max}*e^{-t/\tau}$), with t expressed in days and τ the e-folding time set at 2.88 days. By definition, this empirical parameterisation does not apply to background periods and will not be tested here, but it is available for implementation in CTMs in the absence of more advanced (ecosystem modelling-based) solutions (see ECLAIRE deliverable 4.1).

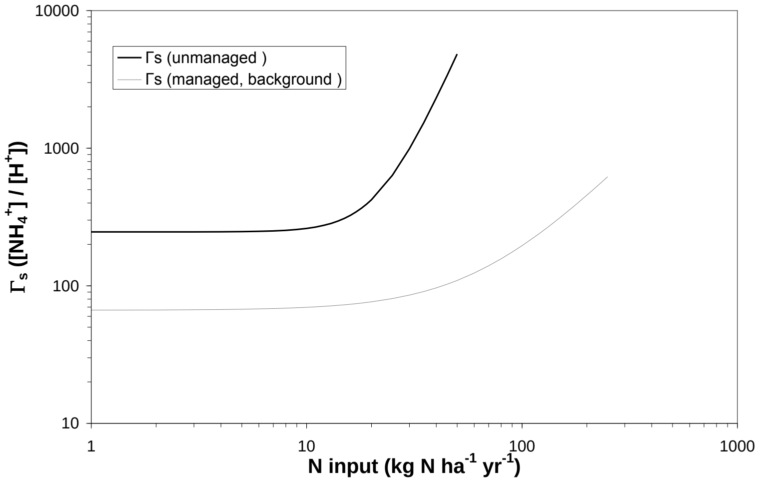


*Figure 2. Relationship of the background stomatal emission potential ($\Gamma_s$) to annual N inputs in the MNS-2010 scheme.*

For $\Gamma_g$ values in background conditions, the MNS-2010 parameterisation scheme proposes that the soil emission potential is treated as negligible wherever there is vegetation (both managed and unmanaged); for periods when soil is bare in agroecosystems (between consecutive crops), $\Gamma_s$ was set to 500.

The non-stomatal resistance to $NH_3$ deposition ($R_w$) was another key model variable investigated, reviewed and parameterised by Massad et al. (2010). The MNS-2010 parameterisation proposes a formulation of $R_w$ that includes an inverse dependence to relative humidity ($NH_3$ uptake is more efficient over wet surfaces), an inverse dependence to an acid/$NH_3$ ratio (AR) index (the more acidic the surface, the more efficient the uptake), and a positive exponential response to temperature (increased temperature will tend to displace dissolved $NH_3$ toward the gas phase, thus reducing uptake rates). The generic default $R_w$ parameterisation was provided in Massad et al. (2010) as:

$$R_w = \frac{R_{w,min}}{LAI^{0.5}} * e^{\alpha(100-RH)} * e^{\beta T} \quad (5)$$

where α is an ecosystem-specific constant (range 0.0318 for forests to 0.176 for grasslands), RH is relative humidity (%), β=0.15, T is surface air temperature (°C), LAI the 1-sided leaf area index, and the minimum value $R_{w,min}$ was given as:

$$R_{w,min} = \frac{\gamma}{AR} \quad (6)$$

with γ = 31.5 s m$^{-1}$ and AR the atmospheric molar concentration ratio calculated from ($HNO_3$+2*$SO_2$+HCl)/$NH_3$.

Figure 3 describes typical variations of $R_w$ over forest as a function of surface relative humidity, ambient acids/$NH_3$ ratio, surface temperature and leaf area index, according to the parameters of Massad et al. (2010). The lowest predicted $R_w$ values (<50 s m$^{-1}$) occur at 100% RH and at the highest AR and LAI values. $R_w$ increases exponentially with decreasing RH, with slope α=0.032 for forests (note that changing α to the value of 0.176 (grassland) results in a much steeper response to RH, with increases in $R_w$ by factors of 2.1, 4.2 and 75.6, at 95%, 90% and 70% RH, respectively, compared with forests). A change in temperature from 5 to 20°C results in a tenfold increase in $R_w$; an increase in LAI from 1 to 5 m$^2$ m$^{-2}$ roughly halves $R_w$ ; and a change in AR from 0.2 ($NH_3$-rich air) to 0.8 ($NH_3$-poor air) decreases $R_w$ by a factor of 4.

A summary table of the parameterisations for Γ and $R_w$ in MNS-2010 is provided in Appendix 1.

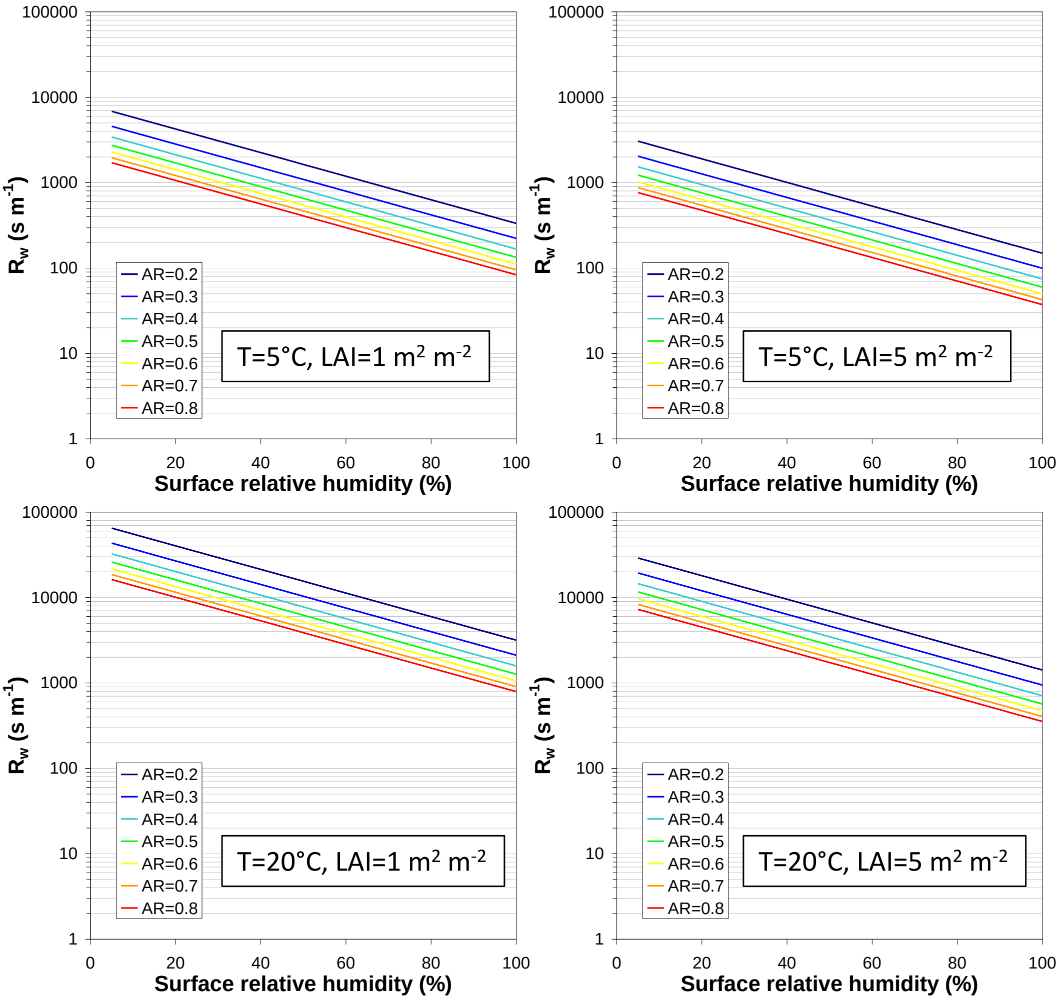


*Figure 3. Variations of the non-stomatal resistance ($R_w$) over forest, as a function of relative humidity, temperature, leaf area index and the acid/$NH_3$ ratio (AR), from the MNS-2010 scheme.*

<u>3.1.2 Evaluation of the MNS-2010 scheme</u>

The MNS-2010 scheme was derived shortly before the start of ECLAIRE from a comprehensive compilation of many $NH_3$ flux datasets worldwide, mostly in the period from the early 1990's to 2010, and can therefore still be considered to represent the state of the art. However, although some of its parameterisations have been adapted for use in the CMAQ-EPIC CTM (Bash et al., 2013), it has not been extensively tested versus actual measured flux datasets at the field scale. This section will show results of model runs applied to "historical" (pre-ECLAIRE) long-term (seasonal to annual) datasets, as well as model applications using measurements from ECLAIRE core sites within Component 1.

The European field sites and associated $NH_3$ flux datasets spanning 20 years, for which the NMS-2001/MNS-2010 model was tested in this Work Package, include the following:

<u>Unfertilised (semi-natural) ecosystems:</u>

- UK-AMO, Auchencorth Moss, extensively grazed moorland, 1995-96-98 (LIFE project)
- NL-Spe, Speulderbos, temperate mixed forest, 2009-10 (NitroEurope), 2013 (ECLAIRE)
- IT-BFo, Bosco Fontana, medit. forest, 2012 (ECLAIRE)

<u>Fertilised agro-ecosystems:</u>

- UK-EBu, Easter Bush, grazed grassland, 2007-08 (NitroEurope)
- CH-Oe1, Oensingen, cut grassland, 2006-07-08-09 (NitroEurope)
- CH-Pos, Posieux, grazed grassland, 2013 (ECLAIRE)
- FR-Gri, Grignon, crop rotation, 2008-09 (NitroEurope), 2012 (ECLAIRE)
- FR-Mej, Méjusseaume, grazed grassland, 2014-2015 (FR-ADEME BTEP project)

The ambient atmospheric $NH_3$ concentrations measured at these sites spanned 6 orders or magnitude, although all concentrations above 100 µg $m^{-3}$ were measured during slurry spreading events (Fig. 4). Median $NH_3$ concentrations over the entire measurement periods at the differents sites were 0.4, 1.9, 2.1, 3.9, 4.3, 4.9, 9.7 and 23.5 µg $m^{-3}$ at UK-AMo, UK-Ebu, CH-Oe1, FR-Mej, NL-Spe, CH-Pos, FR-Gri and IT-BFo, respectively. Note that these concentrations do not necessarily represent the actual annual/multi-annual median concentrations at the sites, as sampling was not continuous but rather focused on specific times of year (e.g. slurry spreading events at FR-Gri). Figure 4 also shows the compared time series of measured $NH_3$ fluxes in the "background" flux range (the large fertiliser-related emission fluxes are not displayed here). The exchange was bi-directional at all sites, but more clearly so at the fertilised agricultural sites (CH-Oe1, CH-Pos, FR-Gri, FR-Mej, UK-Ebu) and at the Dutch high N-deposition Douglas Fir forest (NL-Spe), than at the remote Scottish moorland site (UK-AMo) or the Po Valley forest site (IT-BFo).

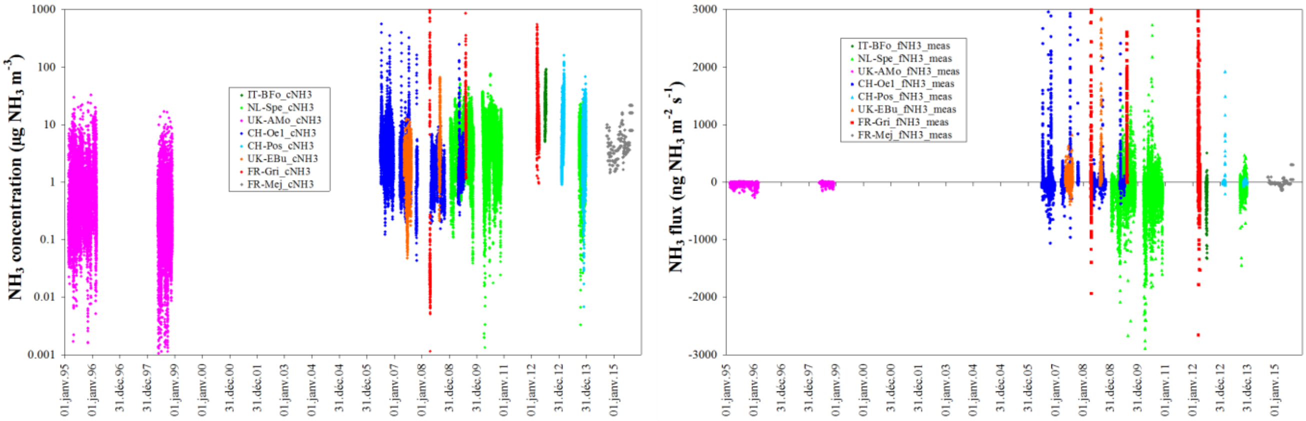


*Figure 4. Overview of measured ambient $NH_3$ concentrations and exchange fluxes at selected European $NH_3$ flux measurement sites. The y-axis on the flux graph has been truncated to display background fluxes only. Concentrations and fluxes were measured on a half-hourly basis using continuous analysers at all sites except at FR-Mej, where data measured using conditional time-averaged gradient (COTAG) systems represent mean values averaged over several days or weeks.*

The parameterised $\Gamma_s$ values according to MNS-2010 are shown in Fig.5, with the lowest apoplastic $\Gamma_s$ ratio (=69) occurring at UK-AMo (Scottish moorland) and the highest $\Gamma_s$ (=3146) at NL-Spe (Dutch forest). The values for fertilised grasslands and croplands are in the range 300-550.

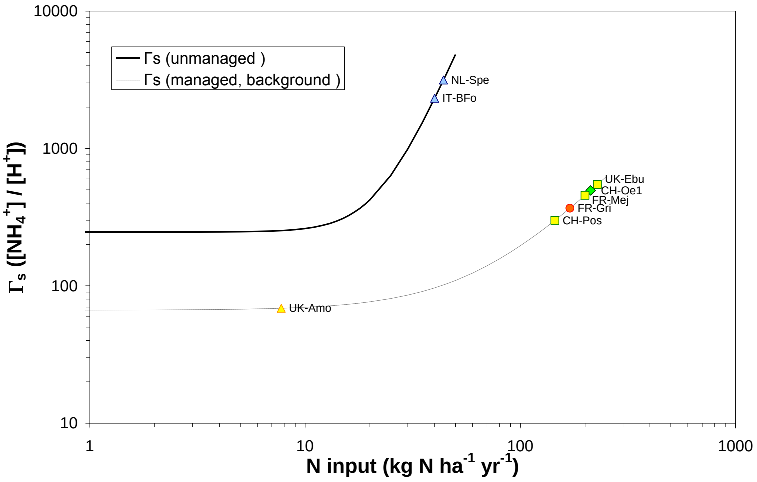


*Figure 5. Parameterised values of $\Gamma_s$ for selected European $NH_3$ flux measurement sites, from the MNS-2010 scheme. Symbols: forests = blue triangles; extensively grazed moorland = yellow triangle; intensively grazed grasslands = yellow squares; cut grassland = green diamond; arable rotation = red circle. Note that the values for the N-fertilised agricultural sites are representative of background periods only (excluding fertilisation episodes).*

The straightforward application, to these selected $NH_3$ flux data sites, of the $R_w$ parameterisation (Eq. 5-6) using MNS-2010 parameters (as in Fig. 3), results in large diurnal and annual variations, driven largely by RH and T. Differences between sites arise from climate but also from LAI and the AR ratio (Fig. 6, left-hand panel). A dominant feature is that $R_w$ never drops below around 30 s $m^{-1}$ at any of the sites, which means that in the case of dry deposition (downward flux) the deposition velocity ($V_d$) never approaches the maximum value allowed by turbulence ($V_{max} = (R_a+R_b)^{-1}$), even though flux observations at certain sites can and do show occurrences of $V_d \sim V_{max}$ (e.g. UK-AMo, Flechard and Fowler, 1998). Another significant feature is that the modelled $R_w$ values systematically reach extremely high values (> $10^5$ s $m^{-1}$) - effectively shutting off the non-stomatal pathway - in even moderately warm and dry conditions, although deliquescent aerosols on leaf surfaces ("micro-wetness") can still sustain a significant sink for atmospheric $NH_3$ (Burkhardt et al., 2009).

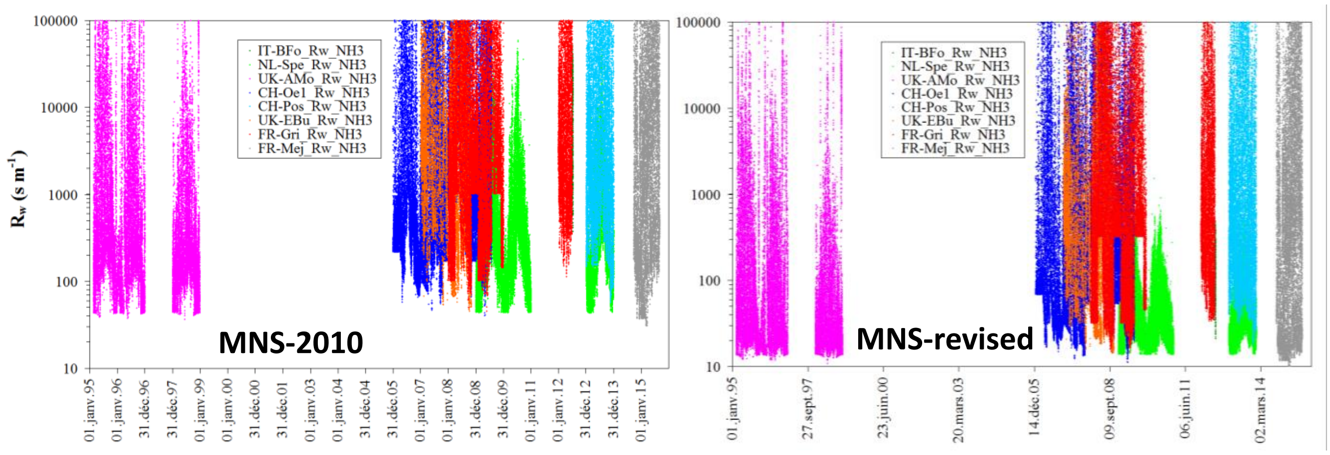


*Figure 6. Parameterised values of $R_w$ for selected European $NH_3$ flux measurement sites, from the MNS-2010 (left) and MNS-revised (right) schemes.*

3.1.2.1 Comparison of MNS-2010 modelled fluxes versus ECLAIRE and other $NH_3$ flux datasets

Modelled $NH_3$ dry deposition fluxes using the default MNS-2010 scheme were systematically underestimated by comparison to measured flux values (see left-hand side panels of both Fig. 7 for unfertilised vegetation and of Fig. 8 for agricultural sites). At the peatland and forest sites (Fig. 7), the average diurnal cycles for different seasons indicate that deposition was underestimated by typically a factor of 5 or 10. During background conditions at the grassland and cropland sites (Fig. 8), deposition was also underestimated to varying degrees, with the largest discrepancy occurring at FR-Gri. Figure 9 shows the same data (each data point is the averaged flux for a certain time of day and in a given month or season, as in Figs. 7-8) displayed as scatter plots and linear regressions for different sites. At three sites (UK-AMo, CH-Oe1 and IF-BFo) there was a reasonably linear relationship and significant correlation between measured and modelled (MNS-2010) fluxes, albeit with regression slopes in the range 0.15-0.53, but at the other three sites there was little correlation between observations and model.

Comparing measured and modelled fluxes at semi-natural sites and at agricultural sites outside fertilisation events means that, in the MNS-2010 parameterisation scheme, the soil emission potential is zero or close to zero, except in the case of grazing (see Appendix 1). Thus the reasons for the observed large underestimation of deposition must be sought in the stomatal emission potential (over-estimated $\Gamma_s$ ?) and/or in the non-stomatal sink strength (over-estimated $R_w$ ?); invoking a larger soil emission potential would only enhance the discrepancy.

A sensitivity analysis applied to these data sets indicated that lowering $\Gamma_s$ values by a significant fraction (e.g. -20%, -50%) would not significantly address the under-deposition issue in the model; there is overall a low sensitivity of the predicted deposition flux to the $\Gamma_s$ value because the stomatal flux is further mediated by stomatal resistance ($R_s$), which is very large (or infinite) in the winter half-year, and still of the order of 100-200 s $m^{-1}$ during the growing season. Further, night-time data (when stomates are almost completely closed, $R_s$ very large) do show a clear underestimation of deposition (Figs. 7-8) at a time when the stomatal emission potential cannot be invoked to explain the discrepancy. This demonstrates that $R_w$ in the MNS-2010 scheme is very likely over-estimated generally and that its parameterisation should be revised.

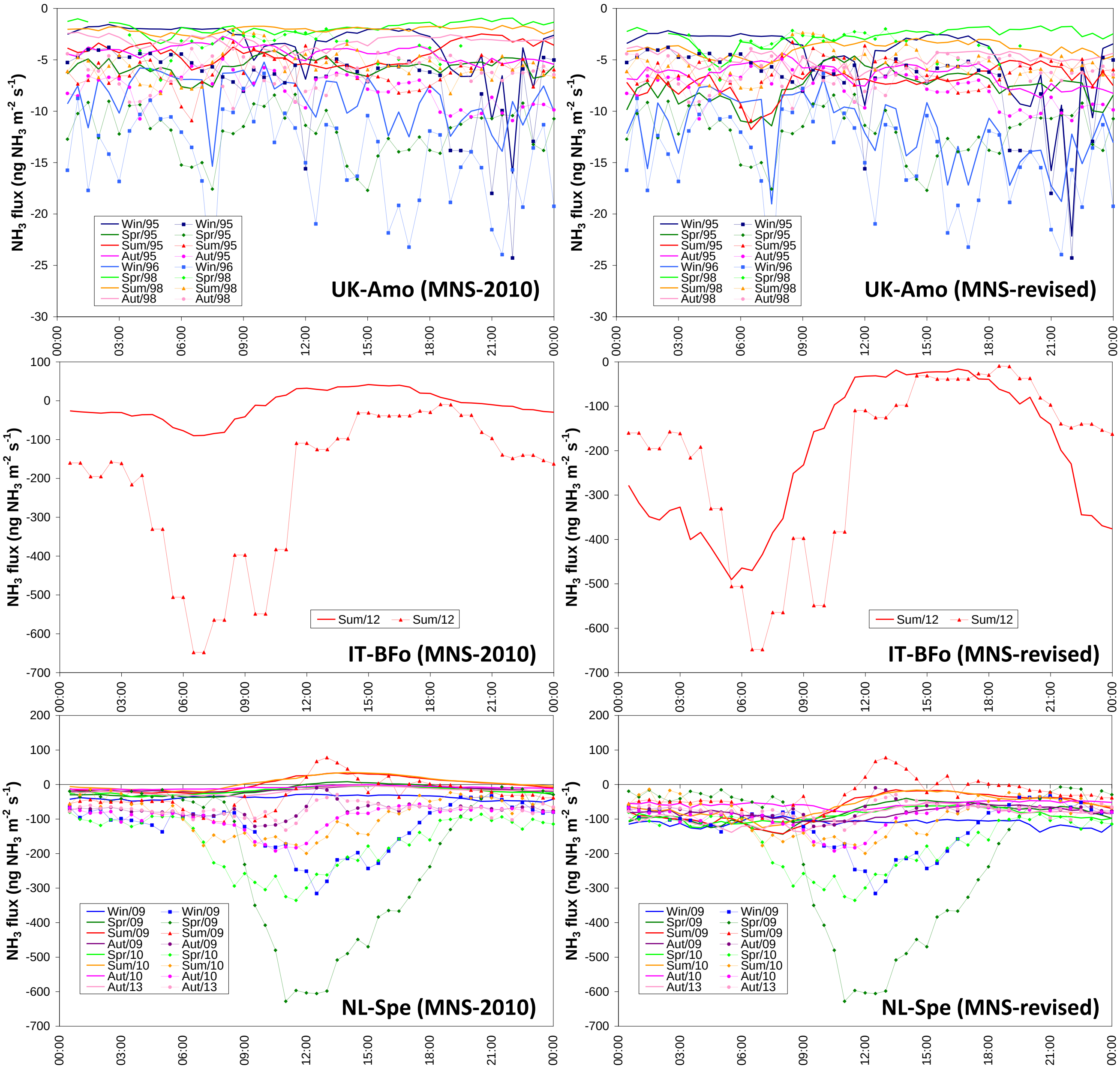


*Figure 7. Comparison of modelled (continuous lines) and measured (dashed lines + symbols) $NH_3$ fluxes at UK-Amo (peatland), IT-BFo (Mediterranean forest) and NL-Spe (Douglas fir forest). Modelled fluxes were simulated using either the default parameters as per MNS-2010 (left-hand side) or revised parameters for $R_w$ (right-hand side) (see text for details).*

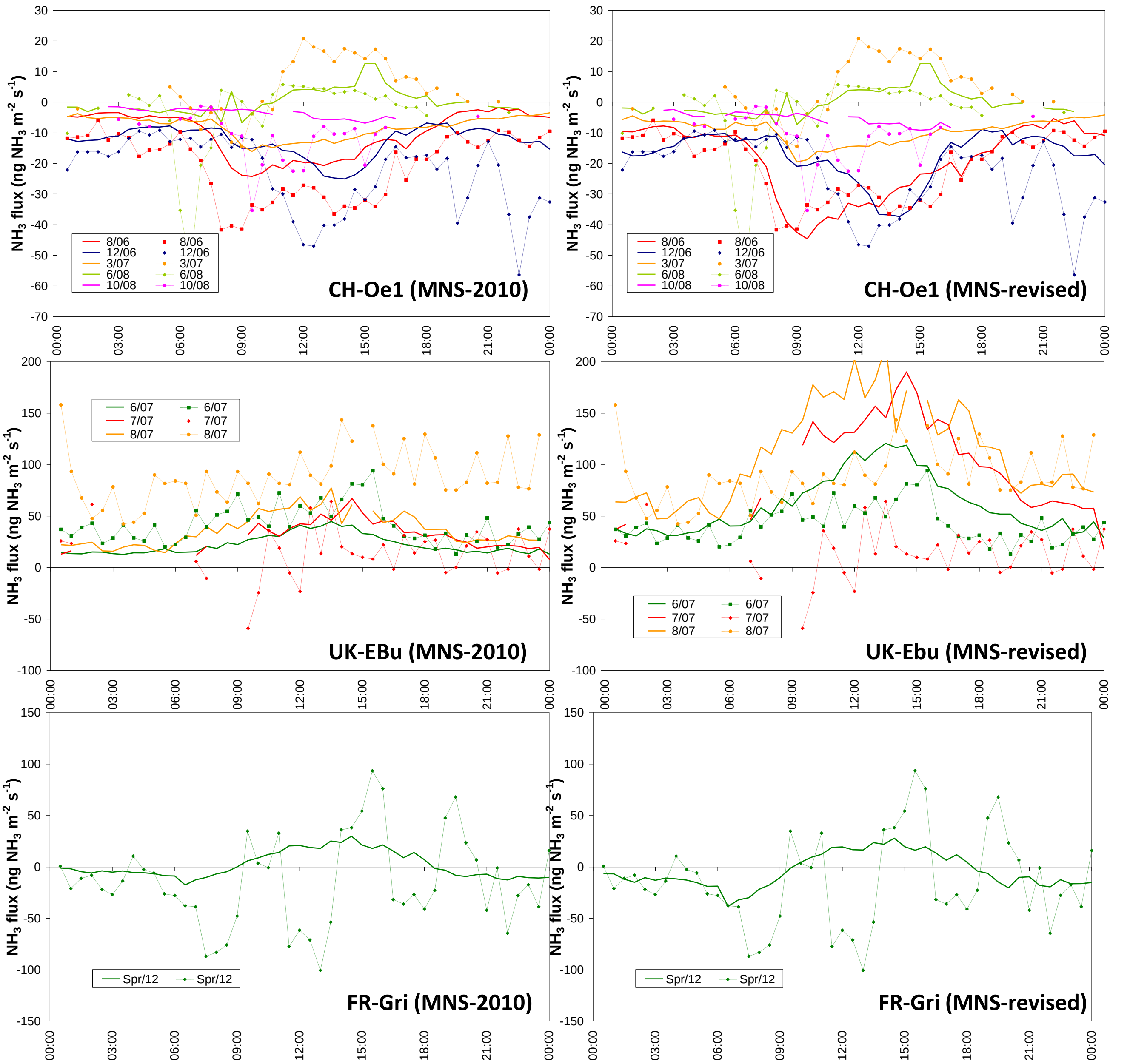


*Figure 8. Comparison of modelled (continuous lines) and measured (dashed lines + symbols) $NH_3$ fluxes at CH-Oe (cut grassland), UK-EBu (grazed pasture) and FR-Gri (crop rotation), during background conditions (fertilisation events were excluded from the datasets). Modelled fluxes were simulated using either the default parameters as per MNS-2010 (left-hand side) or revised parameters for $R_w$ (right-hand side) (see text for details). (Note that for UK-Ebu, in addition to the $R_w$ revision, a revised value of $\Gamma_g$=10000 was introduced for grazing periods, versus $\Gamma_g$=4000 in MNS-2010).*

### 3.1.2.2 Proposed revision of MNS-2010 parameters

For a revised parameterisation of the MNS-2010 scheme (called "MNS-revised" hereafter), we start with the assumptions that i) stomatal emission potentials ($\Gamma_s$) are broadly satisfactorily predicted for background conditions on the basis of the extensive literature review performed by Massad et al. (2010), and ii) the main term responsible for the observed discrepancies to measured fluxes is the non-stomatal sink, characterised by $R_w$.

Figure 6 showed that predicted $R_w$ values in MNS-2010 (left panel of figure) never drop below around 30 s $m^{-1}$, which is not compatible with field observations that occasionally (or frequently, depending on pollution climate) show near-perfect sink behaviour (i.e. near-zero canopy resistance $R_c$~0 s $m^{-1}$, or $V_d$ approaching $V_{max}$). In Eq. (6) and MNS-2010 the minimum non-stomatal resistance $R_{w,min}$ is calculated on the basis of a γ value of 31.5 s $m^{-1}$, which is clearly too high, at least for the set of measurement sites considered here. In parallel, the temperature multiplier (β=0.15 in Eq. 5 and MNS-2010) accounting for the temperature response of $R_w$ leads to an extremely sharp response of $R_w$ (Fig. 3) in daytime and summer.

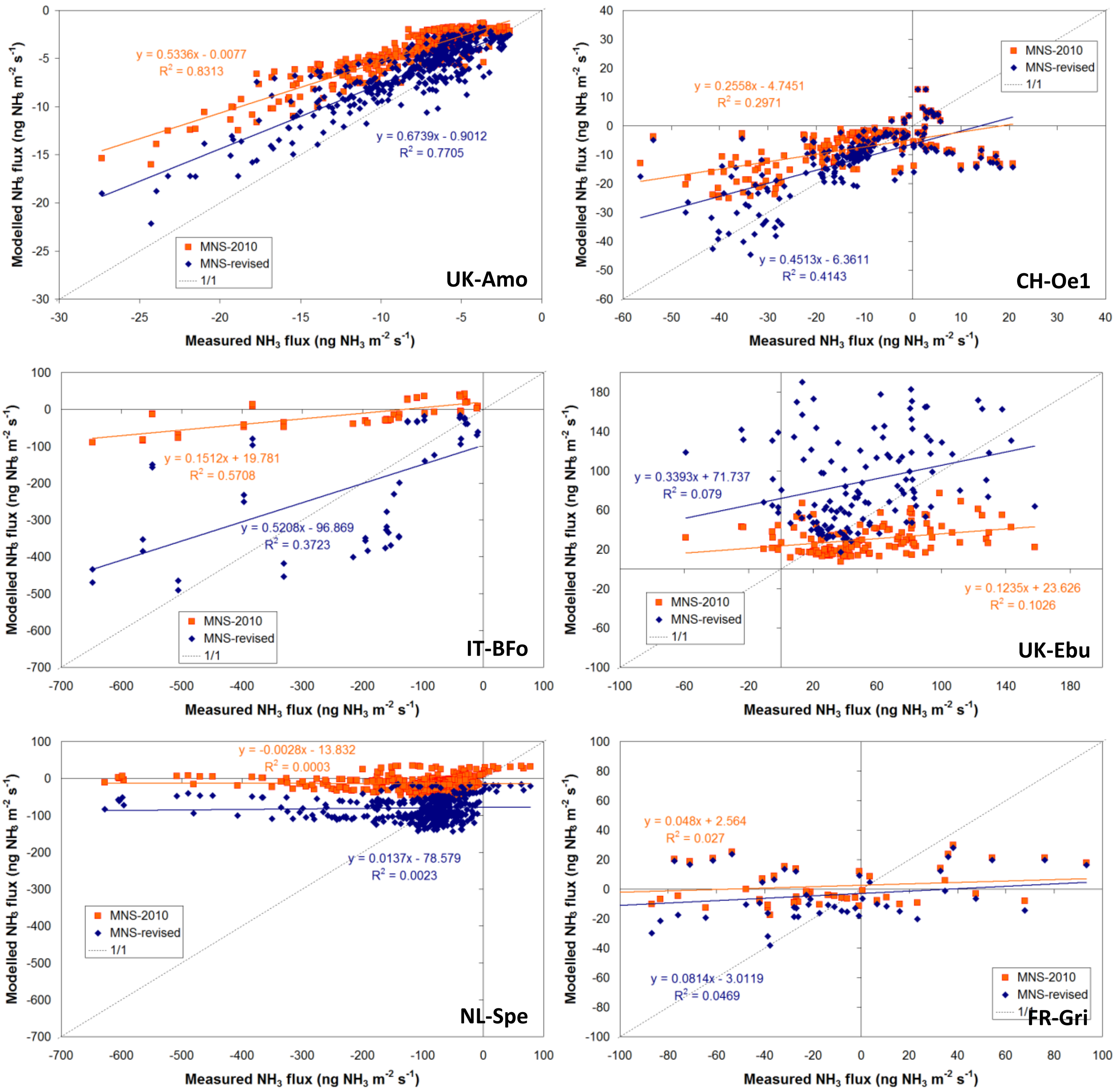


*Figure 9. Scatter plot representation of modelled versus measured fluxes using average diurnal data from Figures 7-8. (Note that for UK-Ebu, in addition to the $R_w$ revision, a revised value of $\Gamma_g$=10000 was introduced for grazing periods).*

The response of the modelled fluxes to changes in the two critical parameters γ and β (Eq. 6) was investigated; a reduction by a factor of 3 for both γ and β (i.e. revised values of γ = 10 s $m^{-1}$ and β = 0.05) resulted in i) a large decrease in $R_w$ (Fig. 6, right-hand panel), and ii) a significant improvement in model results and predictive capability. The MNS-revised model flux results are presented in the right-hand side panels of Figs 7-8, and also in the scatter plots of Fig. 9. The improvement in model performance was especially pronounced at UK-AMo, IF-BFo and CH-Oe1, where model predictions were closest to flux measurements. The model satisfactorily reproduced the diurnal and seasonal patterns of change at UK-Amo and CH-Oe1, with the bi-directional structure well simulated at CH-Oe1. At the Dutch forest site (NL-Spe), the model performance was much improved during night-time (essentially in the flux range from 0 to -150 ng $NH_3$ $m^{-2}$ $s^{-1}$, as shown by the significant improvement in this range in the scatter plot of Fig. 9), which may be taken as a vindication of the revised $R_w$ parameterisation, since the stomatal pathway can be assumed to be negligible at night. However, daytime deposition fluxes in winter and spring remained largely underestimated, while in summer and autumn there was a much better agreement.

At FR-Gri, the improvement in the flux predictions was also manifest during night-time but not during daytime (Fig. 8); however the background flux dataset was of limited duration (around 20 days in March-April 2012), which makes it difficult to evaluate a parameterisation designed for the long-term. This is for example illustrated in the treatment of the impact of the acids to ammonia ratio (AR) on $R_w$ (Eq. 6); here, a long-term average ratio is required to characterize the general pollution climate of the site, while observations made by Loubet et al. (2012) at the FR-Gri site demonstrated the effect on dry deposition fluxes of short-term fluctuations in $SO_2$ and $HNO_3$ in the Paris metropolitan area surrounding the site.

Fluxes from the grazed grassland at UK-EBu are shown in Figs 8-9 alongside the other sites since the fluxes observed during the period shown (summer 2007), in the range -50 to +150 ng ng $NH_3$ $m^{-2}$ $s^{-1}$, can qualify as “background” by contrast to the very sharp and short-lived $NH_3$ emission peaks typically observed after fertilisation. The three summer months in 2007 at UK-Ebu did not contain any organic fertilisation event, but there was sheep grazing (5-2.5 LSU/ha), resulting in small but steady $NH_3$ emissions through the summer. The MNS-2010 scheme assumes a default $\Gamma_g$=4000 for grazed periods (see Appendix 1), which resulted in an under-estimation of emissions (left-hand side panel of Fig. 8). Implementing the change in $R_w$ parameters (as described above) had little impact on modelled fluxes. By contrast, in this case the revision that would be required to bring model results in line with measurements would be a large increase in $\Gamma_g$ (by at least a factor of 2) to better reflect the increased availability of soil $NH_4^+$ through grazing. The right-hand side panel of Fig. 8 shows the mean diurnal emission patterns in measurements and from the model using a revised $\Gamma_g$ value of 10000.

These revised $R_w$ and $\Gamma_g$ parameterisations were further tested on a flux dataset from another grazed grassland (FR-Mej) in background conditions (outside fertilisation events), where long-term $NH_3$ exchange was measured using COTAG systems (Famulari et al., 2010) over several seasons in 2014-2015 (Fig. 10). The measured and modelled datasets show broadly similar patterns of alternating periods of small emissions (during grazing in autumn 2014 and spring 2015) and consistent deposition during winter and also early summer 2015. However, the MNS-2010 scheme tended to underestimate deposition in winter and emission during spring grazing (Fig. 10). With revised $R_w$ and a default $\Gamma_g$ value of 10000, the MNS-revised scheme provides a fair representation of observed fluxes. Since fluxes are integrated over several days or weeks, the COTAG data do not allow for an investigation of diurnal or day to day patterns as for the other sites studied here, but they provide robust long-term flux estimates, which are useful for assessing the MNS parameterisation on yearly time scales.

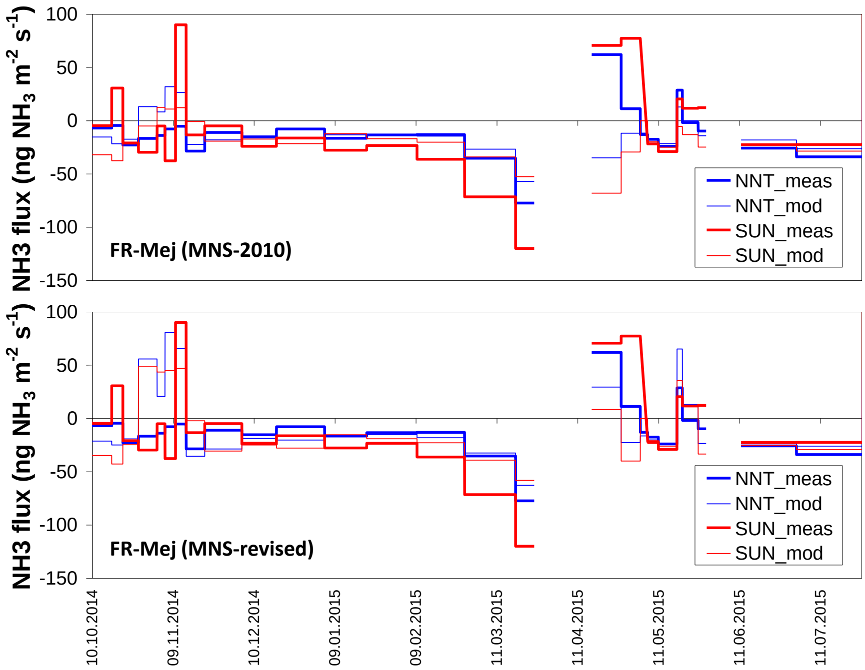


*Figure 10. Seasonal changes in measured (COnditional Time-Averaged Gradient, COTAG, thick lines) and modelled (MNS-2010 and MNS-revised, thin lines) $NH_3$ fluxes over the FR-Mej pasture. The COTAG system provides time-integrated fluxes over periods of several days to weeks, distinguishing near-neutral (NNT) and slightly unstable (SUN) atmospheric conditions. Modelled fluxes were calculated for every half-hour, then averaged over the same NNT and SUN intervals. Grazing occurred late October – early November2014, second half of April and second half of May 2015.*

### *3.2 Meta-modelling of crop emission potentials using CERES-EGC*

#### 3.2.1 Objectives

Within the main objectives of WP3 and WP4: developing updated parameterisation and models for simulating $NH_3$ emissions and improving the description of surface-atmosphere exchange processes for atmospheric pollutants under variable climatic conditions, one of the major challenges was deriving a new set of parameterization for background $NH_3$ emissions. $NH_3$ exchange with the vegetation outside fertilization periods is bi-directional and highly depends on the plant canopy and soil characteristics as well as the climate and air $NH_3$ concentrations (Flechard et al., 2013; Fowler et al., 2009; Massad et al., 2008; Sutton et al., 1995). A logical step towards a better integration of Soil-vegetation $NH_3$ exchange and atmospheric pollutant transport is coupling an ecosystem model and a chemistry and transport model (CTM). This type of online coupling is very challenging due to the complexity of both model types and variety of parameterisations. We propose here a methodology for offline coupling of $NH_3$ background exchange. The methodology is based on the two layer bi-directional $NH_3$ exchange model of Nemitz et al. (2001) and spatial modeling outputs with the CERES-EGC model, where we produce monthly and yearly maps of $\Gamma_g$ and $\Gamma_s$ at the European scale. These maps will either be directly used as input variables to the bi-directional $NH_3$ emissions scheme within a CTM or as a database to construct a meta-model, namely an equation function of the CTM variables, which can be directly incorporated in the CTM.

#### 3.2.2 Methodology for deriving monthly maps of $\Gamma_g$ and $\Gamma_s$

The emission potentials $\Gamma_g$ and $\Gamma_s$ simulations are obtained from runs of the CERES-EGC model for the whole of Europe on a daily time step and with a 0.25°x0.25° grid resolution for three periods: a historical period (1950-2010) and two future periods with two different scenarios RCP4.5 (2010-2100) and RCP8.5 (2010 – 2100).

##### *3.2.2.1 CERES-EGC model*

CERES-EGC is an agro-ecosytem type model which is a version of the CERES family of models (Jones and Kiniry, 1986) adapted to simulate the environmental impacts of crops by Gabrielle et al. (2006). The model is based on several modules each for a different type of crop, but all share the same subroutines for water dynamics, and soil carbon and nitrogen dynamics. At the moment, CERES-EGC simulates the development and growth of several types of agricultural crops namely: maize, wheat, barley, rape, sorghum, sunflower, pea, sugar-beet, soya, and an intercrop (based on the rape crop). The soil organic matter decomposition is based on the NCSOIL model (Gabrielle et al., 2002a; Molina et al., 1983). CERES-EGC runs at a daily time step and for one type of crop at a time. The originality of the model lies in the coupling of a widely used and validated crop growth model (Gabrielle et al., 2002b; Langensiepen et al., 2008; Rezzoug et al., 2008; Xiong et al., 2007) to several environmental impact modules linked to the Nitrogen cycle such as $N_2O$, NO and $NH_3$ emissions.

##### *3.2.2.2 Upscaling method*

Simulations by CERES-EGC are up-scaled by linking the model to a GIS database. The GIS database used for the model entry data is detailed below. The model runs independently for each grid cell and for consecutive 150 years of simulations.

**Soil database.** The soil data were extracted from the European soil database (Panagos et al., 2012) and were aggregated on the 0.25°x0.25° grid. Several soil parameters necessary to run the CERES-EGC model were derived from pedotransfer functions (Ritchie, 1972). Figure 11 below shows the European map of the soil top layer pH values as used by the model simulations and further $\Gamma_g$ calculations.

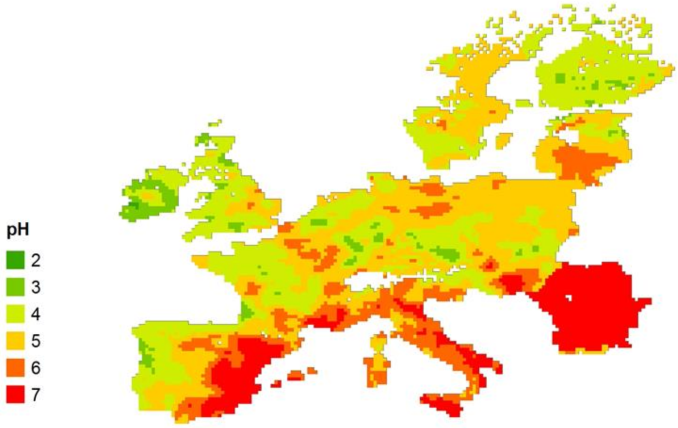


*Figure 11. Soil pH values for the soil top layer used for model simulations and $\Gamma_g$ calculations.*

**Management data.** Data were extracted from the open access GHG-Europe project database and were initially provided by M. Wattenbach. The data contains the crop sequences from 1976 to 2010, the total yearly amount of nitrogen and the repartition in organic and mineral nitrogen on a 1 x 1 km grid. The data were aggregated on a 0.25°x0.25° grid by selecting the two major rotations from the pixels lying within this grid cell. Those two rotations represented on average 70% of the grid cell. Additional data such as dates of application of N fertilizer and sowing of crops were calculated from simple algorithms based on minimal and maximal temperature requirements, precipitation conditions as well as selected date intervals for each crop based on standard European management practice. Figure 12 below illustrates the total nitrogen fertilization used for 2005 as an input variable for the CERES-EGC simulation.

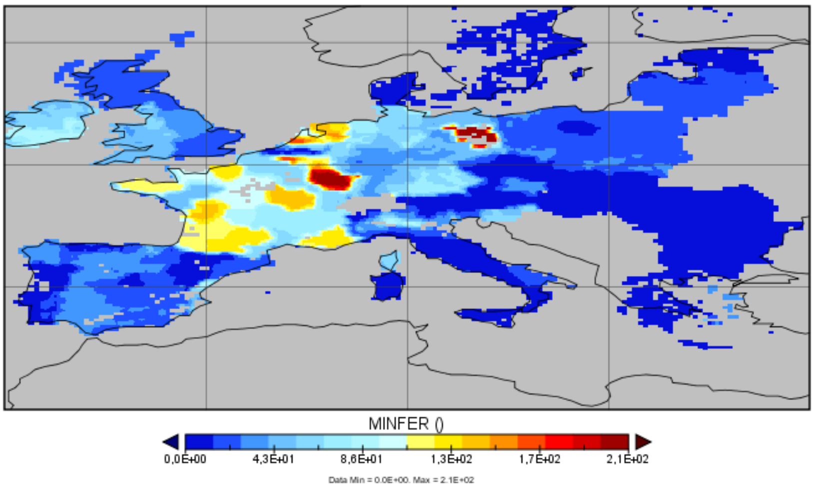


*Figure 12. Total mineral fertilization application map in kg ha$^{-1}$ as used as input for model simulations.*

**Climate data.** Meteorological data are derived from the HadGEM2-ES climate model for two scenarios as described above (RCP 4.5 and RCP 8.5). The variables needed to run the EGC-model on a daily time step are: Maximum and minimum daily temperatures (°C), Cumulated daily precipitation (mm), Average daily Short wave radiation (W m$^{-2}$), and average daily wind speed (m s$^{-1}$).

### *3.2.2.3 Emission potential calculations*

**Soil emission potential.** $\Gamma_g$ is defined as the soil ammonia emission potential and can be calculated using the equation below:

$$\Gamma_g = \frac{[NH_4^+]_{soil}}{[H^+]_{soil}} \quad (7)$$

Where $[NH_4^+]_{soil}$ is the top layer soil ammonium concentration in mol $L^{-1}$ as simulated by the CERES-EGC model and $[H^+]_{soil}$ is derived from the soil pH map for the top layer. Note that the CERES-EGC outputs are given in gram N-NH4+ per hectare. We therefore use the simulated soil water content of the soil top layer and the Soil bulk density to transform the $NH_4^+$ concentration into mol $L^{-1}$. [see note[1]]

**Stomatal emission potential.** Otherwise called $\Gamma_s$ is the stomatal emission potential which can be calculated from the equation below:

$$\Gamma_s = \frac{[NH_4^+]_{apo}}{[H^+]_{apo}} \quad (8)$$

where $[NH_4^+]_{apo}$ and $[H^+]_{apo}$ are the apoplastic $NH_4^+$ concentrations and apoplastic pH respectively. These two variables are not simulated by the CERES-EGC model; however the model simulated $NH_4^+$ concentrations in g g-1 dry weight which we use as a proxy to estimate total plant $NH_4^+$ content and use the equation below from Massad et al. (2010) to estimate $\Gamma_s$:

$$\Gamma_s = 19.3 \times e^{0.0506 \times [NH_4^+]_{bulk}} \quad (9)$$

where $NH_4^+{}_{bulk}$ is the total plant ammonium concentration in µg $NH_4^+$ $g^{-1}$ tissue fresh weight. We assume that the ratio of fresh weight to dry weight of the leaves is equal to 10.

### 3.2.4 Methodology for developing the meta-modelling concept of background $\Gamma_g$ in Europe

The simulations of CERES-EGC $\Gamma_g$ were used to retrieve a meta-model of $\Gamma_g$. Such a meta-model is useful as it is a simple representation of a complex model which can be included in a chemical transport model. The objective here is to develop a model of the $\Gamma_g$ which is representative of the background conditions, away from any fertilization events, as the $\Gamma_g$ following fertilization was developed based on the Volt'air model dedicated to such conditions, while the processes in CERES-EGC are not well adapted to reproduce these conditions. However, since CERES-EGC simulations include fertilization events, we used despiked yearly averaged $\Gamma_g$ to evaluate the background $\Gamma_g$ meta-model as detailed below.

The methodology used for finding the $\Gamma_g$ meta-model was similar as the one used in D3.1 and D4.1. Monthly means of ($\Gamma_g^{CERES}$) were retrieved from the CERES-EGC computations in each 0.25°×0.25° grid cell in Europe, together with the drivers of the model (soil and meteorological data and nitrogen fertilization rates) for the year 2005. Extreme values of $\Gamma_g$ were filtered out by a regressive despiking algorithm. All data were then averaged over the entire year. Then a multiple linear regression was performed between the logarithm of $\Gamma_g^{CERES}$ and the other variables in the dataset, to find $\Gamma_g^{meta-model}(bgd)$ which satisfies:

$$ln\left(\Gamma_g^{meta-model}(bgd)\right) = \left[a_0 + \sum_{1:m} a_i x_i(site, period)\right] \quad (10)$$

where $a_0 \cdots a_m$ are the model coefficients and $x_1 \cdots x_m$ are the yearly averaged soil, meteorological and fertilisation variables which are by nature dependent on the sites and periods. The linear regression

1 $$[NH_4^+]_{soil} = \frac{NH4_{1\left(\frac{kg}{ha}\right)}}{M_{mol\,N}\left(\frac{g}{mol}\right) \times 10^{-3} \times \frac{SWC_{1(\%vol)}}{100} \times \frac{depth_{1(cm)}}{100} \times 10^3\left(\frac{L}{m^3}\right) \times 10^4\left(\frac{m^2}{ha}\right)}$$

retrieves the $a_0 \cdots a_m$ coefficients that minimize the mean square error of the logarithms using the linear model (*lm*) function in *R*:

$$MSE = \frac{1}{N}\sum_{European\ pixels}\left[ln\left(\Gamma_g^{meta-model}\right) - ln\left(\Gamma_g^{CERES}\right)\right]^2 \quad (11)$$

The best model performance was retrieved with a stepwise algorithm that maximises the Akaïke *An Information Criterion* (AIC = $-2ln(L) - 2(N_P + 1)$, where $L$ is the likelihood and $N_P$ the number of parameters of the model.

## 3.2.5 Results of the CERES-EGC modelling of $NH_3$ emission potentials

We present here results for $\Gamma_g$ and $\Gamma_s$ calculations based on spatial CERES-EGC outputs for the year 2005 and for the year 2050 based on two different climate scenarios RCP4.5 and RCP8.5.

### *3.2.5.1 Yearly dynamics of $NH_3$ emission potentials*

Figure 13 illustrates the box plot for the yearly dynamics of all pixels of the European domain for $\Gamma_g$. The simulated values for $\Gamma_g$ for background conditions vary between 50 and 6000 and lie within reported values in literature (Flechard et al., 2013; Massad et al., 2010). The yearly dynamics of the means and medians are however very small but could be explained by the bias of looking at monthly means of $\Gamma_g$. Peak $\Gamma_g$ values are usually very temporary and only last a few days as given for example in Massad et al. (2010) with an exponential decrease and a decaying time of 2.8 days.

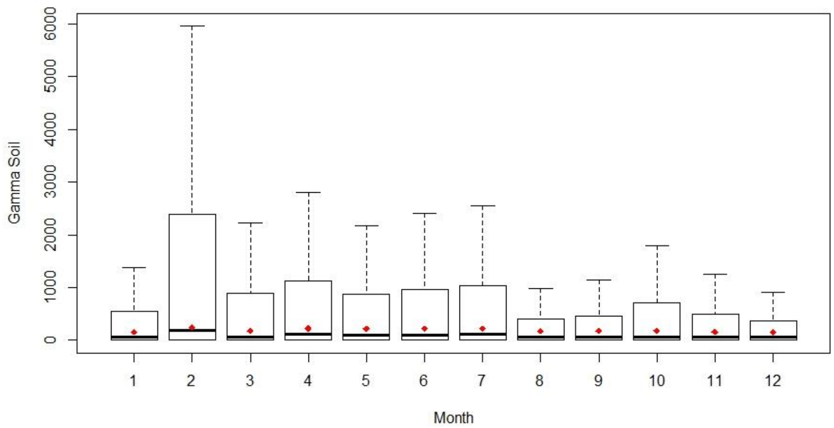


*Figure 13. Box plot of yearly dynamics of $\Gamma_g$ for the year 2005. Red dots represent means.*

A similar pattern is noted also for $\Gamma_s$ values as illustrated in Figure 14 below where monthly means and medians present little variability. Simulated $\Gamma_s$ vary between 20 and 250 and are also in line with expected values as noted in the literature. We notice however a different distribution where maximum values are in the cold months and minimal values in warm months. This could be an artefact of the calculation we used since simulated $NH_4^+$ concentrations are normalized by the total biomass of the plant and months 11, 12, 1, 2 and 3 shows the lowest yearly biomass values.

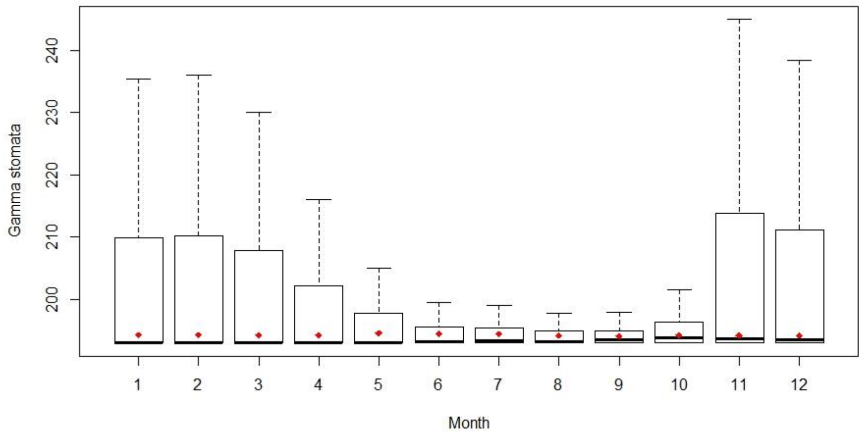


*Figure 14. Box plot of yearly dynamics of $\Gamma_s$ for the year 2005. Red dots represent means.*

*3.2.5.2 Spatial variability of $\Gamma_g$ and $\Gamma_s$*

The spatial variability of $\Gamma_g$ values is tightly correlated to that of the soil pH values as illustrated in Figure 15 for the year 2005 with low values in acidic soils and high values in alkaline soils.

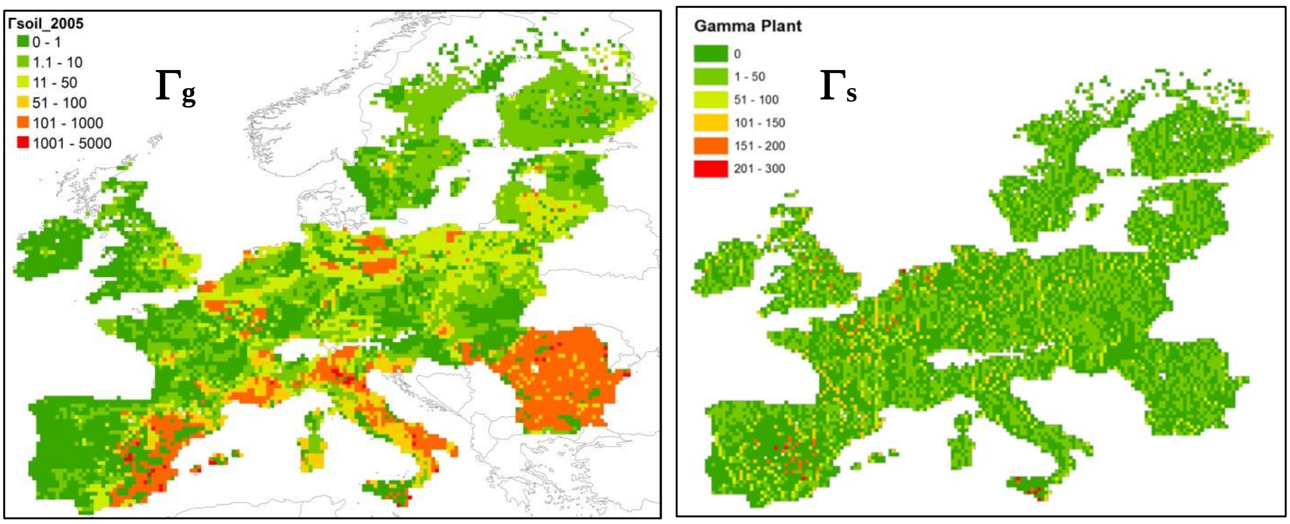


*Figure 15. Spatial distribution of yearly average $\Gamma_g$ and $\Gamma_s$ values for 2005. Note that the two scales are different. The large $\Gamma_g$ values in Bulgaria and Romania are due to default soil pH set to 7.*

Concerning $\Gamma_s$, we notice a homogenous distribution on the entire domain (Figure 15) with some hot spots in France and Spain but with generally weak values. This is explained by the fact that plant $NH_4^+$ concentrations as modelled by CERES are a result of soil available $NH_4^+$ and plant demand which is a result of plant growth and therefore availability of Nitrogen and are therefore not very variable. An improvement of this modelling exercise would be to better parameterize plant roots absorption of $NH_4^+$ after the fertilization events when the absorption of the plant is peaking (Husted et al., 1996; Massad et al., 2009).

*3.2.5.3 Effect of climate change on of $NH_3$ emission potentials*

Figure 16 illustrates the difference between yearly averages for 2050 between the two climatic scenarios RCP8.5 and RCP5.5 for $\Gamma_g$ and $\Gamma_s$ respectively.

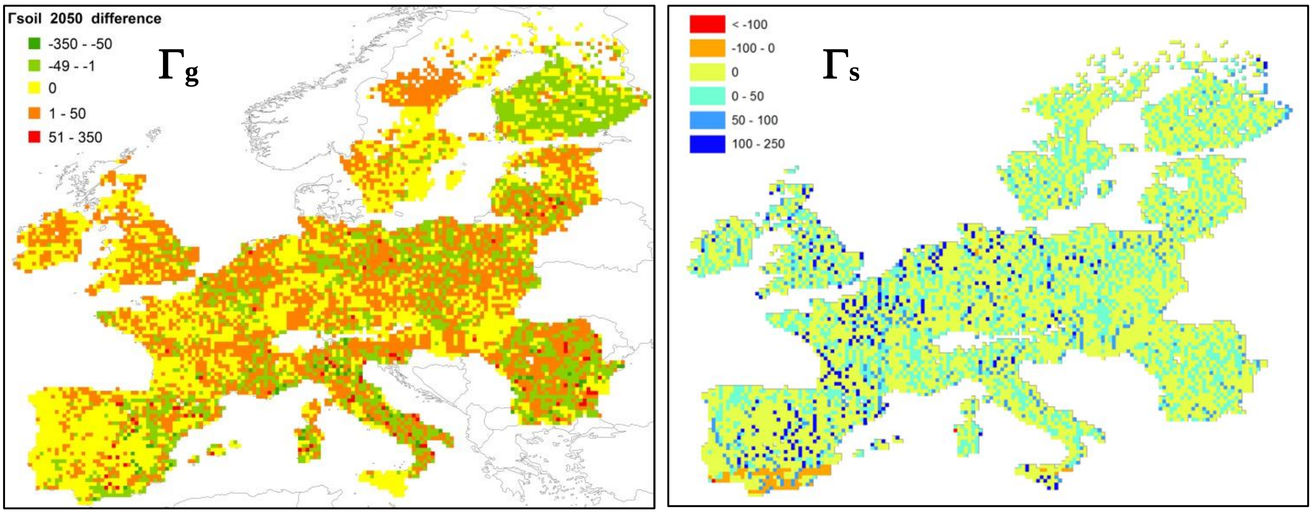


*Figure 16. Difference in yearly $\Gamma_g$ and $\Gamma_s$ plant averaged for 2050 between two climatic scenarios RCP8.5 and RCP4.5. Note the different scales.*

We notice an increase in $\Gamma_g$ values with RCP8.5 scenario, especially for northern regions. This can partly be explained by the effect on soil water content in the soil top layer that affects the calculation of $\Gamma_g$. Concerning $\Gamma_s$, we notice a decrease for the RCP8.5 scenario as compared to the RCP4.5 scenario except for the south of Spain. This could be explained by an increase in plant growth and therefore an increase in plant N uptake except where plants are water stressed and therefore growth is limited.

3.2.6 Results of the meta-modelling concept of background $\Gamma_g$ in Europe

These results show the first attempt to retrieve the background $\Gamma_g$ meta-model for European conditions.

*3.2.6.1 Meta-model parameters and performance*

Two meta-models were tested, one with the most available meteorological and soil variables (Model 1) and the second with only soil pH and yearly fertilization (Model 2; Table 1). The meta-modelling approach was quite successful as shown by the quite high efficiency values (Table 2), although the RRMSE > 1 indicate that the $\Gamma_g$ is correctly represented by the meta-model within roughly 60%. Nevertheless, bearing in mind the considerable range of $\Gamma_g$ values, from below $10^{-1}$ to more than $10^3$, it is clear that the meta-models reproduce the order of magnitude of $\Gamma_g$ in Europe correctly as shown by Figure 17.

**Table 1. Coefficient values of the meta-models 1 and 2 of $ln\left(\Gamma_g^{meta-model}\right)$. The meteorological and soil variables are yearly averages.**

| Coefficient | Model 1 | | Model 2 | |
|---|---|---|---|---|
| | Estimate | Std. Error | Estimate | Std. Error |
| $a_0$ | -9.78 | 0.086 | -10.3 | 0.06 |
| Minimum daily temperature (°C) | 0.028 | 0.0004 | - | - |
| Maximum daily temperature (°C) | -0.059 | 0.008 | - | - |
| Daily precipitation (mm) | -0.004 | 0.008 | - | - |
| *ln*(annual Fertilisation in kg N $ha^{-1}$) | 0.39 | 0.007 | 0.37 | 0.007 |
| Soil pH | 2.22 | 0.010 | 2.16 | 0.01 |

**Table 2: Quality of fit of the meta-models 1 and 2 of background $\Gamma_g$ for Europe. Model 1 incorporates all variables while Model 2 only uses fertilisation rate and soil pH. RMSE = Root Mean Square Error, RRMSE = Relative Root Mean Square Error, MAE = Mean Average Error, RMAE = Relative Mean Average Error, EF = Efficiency**

| | Model 1 | Model 2 |
|---|---|---|
| RMSE | 135 | 134 |
| RRMSE | 1.61 | 1.60 |
| MAE | 44 | 44 |
| RMAE | 0.52 | 0.53 |
| Bias | 4.9 | 4.8 |
| EF | 0.56 | 0.56 |

The parameters of the meta-model of $\Gamma_g$ (Table 1) show that, as expected, $\Gamma_g$ is responding positively to soil pH and nitrogen fertilisation. It is also positively correlated with minimum daily temperature, while it is negatively correlated with precipitation (which leads to more dilution of the soil ammonium in soil water) and maximum temperature. Overall the response to temperature is negative because the coefficient of maximum daily temperature is larger than that of the minimum temperature. Hence the response of the mean temperature will be negative.

The main drivers of $\Gamma_g$ are however fertilization and soil pH, as shown by the overall good performance of the Model 2, which only uses these two variables. The corresponding simplified model gives the yearly averaged background $\Gamma_g$ in the form:

$$\Gamma_g^{bgd} \sim \alpha \times {N_{applied}}^{0.37} \times e^{2.16pH_{soil}} \quad (11)$$

Where $N_{\mathrm{applied}}$ is in kg N $ha^{-1}$. Equation 11 however does not show any response to temperature, which means that in first order, $\Gamma_g$ will not respond to climate change. The response to temperature and precipitation would however be of the following form:

$$\Gamma_g^{bgd} \sim \alpha \times e^{-0.03T} \times e^{-0.004P} \quad (12)$$

These equations have to be taken with caution as they have to be validated prior to being used. It is nevertheless demonstrated how new parameterisation in the MNS 2010 approach can be deduced from CERES-EGC modelling at European scale (see Table in Appendix 1 where $\Gamma_g$ is unknown).

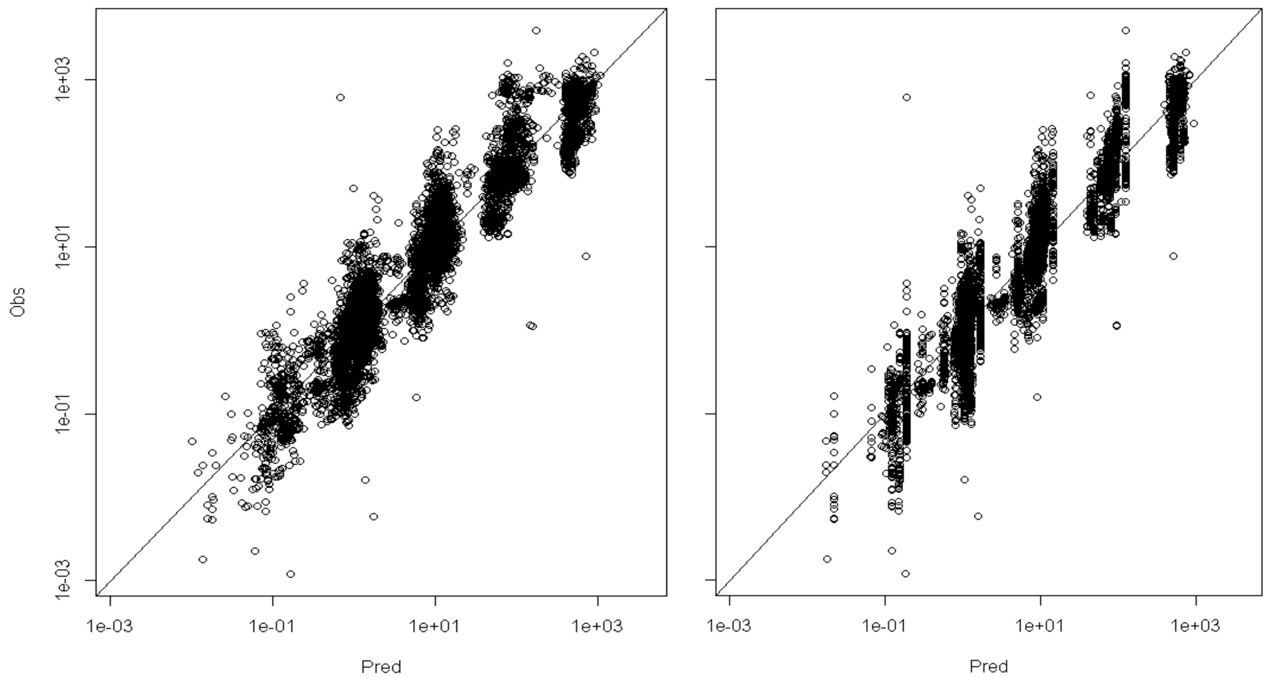


*Figure 17. Observed (CERES-EGC) versus predicted (meta-model) yearly averaged $\Gamma_g$ in Europe. Left: Model 1. Right: Model 2.*

## 4. Results:

This deliverable has provided improved parameterisations for background bi-directional $NH_3$ exchange with soil and vegetation, based on extensive testing and calibration and/or meta-modelling using state-of-the-art models:

- the Massad-Nemitz-Sutton (2010) parameterisation for semi-natural and background agricultural vegetation, for stomatal exchange and non-stomatal uptake;
- the CERES-EGC crop model for meta-modelling of the background soil emission potential;
- A proof of concept for developing a meta-model of soil emission potential based on yearly averages.

The MNS parameterisation was found to provide realistic $NH_3$ exchange estimates over a range of semi-natural and agricultural sites in background conditions, with minimal adjustments required for some parameters. More field-scale testing using a wider range of flux datasets, as well as regional-scale testing within chemical transport models could further refine the model's calibration, but the scheme already shows good potential for a generalised implementation in CTMs. Some areas could be further improved, such as the characterisation of ground-layer emissions from decomposing leaf litter, even in unfertilised ecosystems (e.g. Hansen et al., 2013).

We proved the concept of using the CERES-EGC modelling approach for retrieving soil and plant ammonia emission potentials. Preliminary results are satisfactory in the sense that values are consistent with values reported in the literature. We present a first analysis based on monthly averages which needs to be refined with respect to temporal variability as it would be more conclusive to look at daily values. These maps can be used as input variables to chemistry and transport models to simulate the effect of different climate change scenarios or land use change scenarios.

We showed that the approach of developing a meta-model of the soil emission potential was suitable and could lead to simple formulation of this potential in background conditions in Europe. Further developments should include monthly variations of the soil emission potential and species specific analysis.

## 5. Milestones achieved:

MS12: Summary report (on site applications of improved NH3/NO and VOC models, including uncertainty assessment and comparison with original approaches)

MS13: Provision of site based estimates of NH3/NO and VOC exchange for ÉCLAIRE core sites for present and future environmental conditions

## 6. Deviations and reasons:

This deliverable was due Month 30 and was delayed Month 48. We had planned to base our work on the ESX model framework, which led to an initial delay in delivery. However ultimately we changed our strategy (after Month 36) to develop an approach based on the improvement of the parameterisations of the MNS 2010 modelling framework.

## 7. Publications:

Carozzi, M., Loubet, B., Acutis, M., Rana, G. and Ferrara, R.M., 2013. Inverse dispersion modelling highlights the efficiency of slurry injection to reduce ammonia losses by agriculture in the Po Valley (Italy). Agric. For. Meteorol., 171–172(0): 306-318.

Cellier, P., Rochette, P., Henault, C., Genermont, S., Laville, P. and Loubet, B., 2013. Gaseous emissions at different space scales in the nitrogen cycle: A review. Cahiers Agricultures, 22(4): 258-271.

Ferrara R.M., Loubet B., Decuq C., Palumbo A.D., Di Tommasi P., Magliulo V., Masson S., Personne E., Cellier P., Rana G., 2014. Ammonia volatilisation following urea fertilisation in an irrigated sorghum crop in Italy. Agricultural and Forest Meteorology, 195-196, 179-191.

Flechard, C.R., Massad, R.-S., Loubet, B., Personne, E., Simpson, D., Bash, J.O., Cooter, E.J., Nemitz, E. and Sutton, M.A. 2013. Advances in understanding, models and parameterisations of biosphere-atmosphere ammonia exchange, Biogeosciences 10, 5183–5225.

Fowler, D., Steadman, C.E., Stevenson, D., Coyle, M., Rees, R.M., Skiba, U.M., Sutton, M.A., Cape, J.N., Dore, A.J., Vieno, M., Simpson, D., Zaehle, S., Stocker, B.D., Rinaldi, M., Facchini, M.C., Flechard, C.R., Nemitz, E., Twigg, M., Erisman, J.W. and Galloway, J.N., 2015. Effects of global change during the 21st century on the nitrogen cycle. Atmos. Chem. Phys. Discuss., 15(2): 1747-1868.

Garcia, L., Genermont, S., Bedos, C., Simon, N.N., Garnier, P., Loubet, B. and Cellier, P., 2012. Accounting for Surface Cattle Slurry in Ammonia Volatilization Models: The Case of Volt'Air. Soil Science Society of America Journal, 76(6): 2184-2194.

Loubet, B., Decuq, C., Personne, E., Massad, R.S., Flechard, C., Fanucci, O., Mascher, N., Gueudet, J.C., Masson, S., Durand, B., Genermont, S., Fauvel, Y. and Cellier, P., 2012. Investigating the stomatal, cuticular and soil ammonia fluxes over a growing tritical crop under high acidic loads. Biogeosciences, 9(4): 1537-1552.

Personne, E., Tardy, F., Génermont, S., Decuq, C., Gueudet, J.-C., Mascher, N., Durand, B., Masson, S., Lauransot, M., Fléchard, C., Burkhardt, J. and Loubet, B., 2015. Investigating sources and sinks for ammonia exchanges between the atmosphere and a wheat canopy following slurry application with trailing hose. Agric. For. Meteorol., 207: 11-23.

Simpson, D., Benedictow, A., Berge, H., Bergstrom, R., Emberson, L.D., Fagerli, H., Flechard, C.R., Hayman, G.D., Gauss, M., Jonson, J.E., Jenkin, M.E., Nyiri, A., Richter, C., Semeena, V.S., Tsyro, S., Tuovinen, J.P., Valdebenito, A. and Wind, P., 2012. The EMEP MSC-W chemical transport model - technical description. Atmospheric Chemistry and Physics, 12(16): 7825-7865.

Sintermann, J., Neftel, A., Ammann, C., Hani, C., Hensen, A., Loubet, B. and Flechard, C.R., 2012. Are ammonia emissions from field-applied slurry substantially over-estimated in European emission inventories? Biogeosciences, 9(5): 1611-1632.

Sutton, M.A., Reis, S., Riddick, S.N., Dragosits, U., Nemitz, E., Theobald, M.R., Tang, Y.S., Braban, C.F., Vieno, M., Dore, A.J., Mitchell, R.F., Wanless, S., Daunt, F., Fowler, D., Blackall, T.D., Milford, C., Flechard, C.R., Loubet, B., Massad, R., Cellier, P., Personne, E., Coheur, P.F., Clarisse, L., Van Damme, M., Ngadi, Y., Clerbaux, C., Skjoth, C.A., Geels, C., Hertel, O., Kruit, R.J.W., Pinder, R.W., Bash, J.O., Walker, J.T., Simpson, D., Horvath, L., Misselbrook, T.H., Bleeker, A., Dentener, F. and de Vries, W., 2013. Towards a climate-dependent paradigm of ammonia emission and deposition. Philos. Trans. R. Soc. B-Biol. Sci., 368(1621).

## 8. Meetings:

March 2012, CEH, Edinburgh. WP4 meeting, launch of ESX idea

May 2013, Univ. Bonn. WP4-ESX meeting

May 2014, CEH Edinburgh. Joint C1-ESX meeting

## 9. List of Documents/Annexes:

Appendix 1: Summary of the MNS-2010 parameterisation of a two-layer NH3 bi-directional exchange model (Massad et al., 2010).

## 10. References

Bash, J. O., Cooter, E. J., Dennis, R. L., Walker, J. T., and Pleim, J. E.: Evaluation of a regional air-quality model with bidirectional NH3 exchange coupled to an agroecosystem model, Biogeosciences, 10, 1635–1645, doi:10.5194/bg-10-1635-2013, 2013.

Burkhardt, J., Flechard, C. R., Gresens, F., Mattsson, M., Jongejan, P. A. C., Erisman, J. W.,Weidinger, T., Meszaros, R., Nemitz, E., and Sutton, M. A.: Modelling the dynamic chemical interactions of atmospheric ammonia with leaf surface wetness in a managed grassland canopy, Biogeosciences, 6, 67–84, doi:10.5194/bg-6-67-2009, 2009.

Famulari, D., Fowler, D., Nemitz, E., Hargreaves, K. J., Storeton-West, R. L., Rutherford, G., Tang, Y. S., Sutton, M. A., and Weston, K. J.: Development of a low-cost system for measuring conditional time-averaged gradients of $SO_2$ and $NH_3$, Environ. Monit. Assess., 161, 11–27, doi:10.1007/s10661-008-0723-6, 2010.

Flechard, C. R. and Fowler, D.: Atmospheric ammonia at a moorland site. II: Long-term surface-atmosphere micrometeorological flux measurements, Q. J. Roy. Meteor. Soc., 124, 759–791, 1998.

Flechard, C. R., Massad, R.-S., Loubet, B., Personne, E., Simpson, D., Bash, J. O., Cooter, E. J., Nemitz, E., and Sutton, M. A.: Advances in understanding, models and parameterizations of biosphere-atmosphere ammonia exchange, Biogeosciences, 10, 5183–5225, doi:10.5194/bg-10-5183-2013, http://www.biogeosciences.net/10/5183/2013/, 2013.

Fowler, D., Pilegaard, K., Sutton, M.A., Ambus, P., Raivonen, M., Duyzer, J., Simpson, D., Fagerli, H., Fuzzi, S., Schjoerring, J.K., Granier, C., Neftel, A., Isaksen, I.S.A., Laj, P., Maione, M., Monks, P.S., Burkhardt, J., Daemmgen, U., Neirynck, J., Personne, E., Wichink-Kruit, R., Butterbach-Bahl, K., Flechard, C., Tuovinen, J.P., Coyle, M., Gerosa, G., Loubet, B., Altimir, N., Gruenhage, L., Ammann, C., Cieslik, S., Paoletti, E., Mikkelsen, T.N., Ro-Poulsen, H., Cellier, P., Cape, J.N., Horvath, L., Loreto, F., Niinemets, A., Palmer, P.I., Rinne, J., Misztal, P., Nemitz, E., Nilsson, D., Pryor, S., Gallagher, M.W., Vesala, T., Skiba, U., Bruggemann, N., Zechmeister-Boltenstern, S., Williams, J., O'Dowd, C., Facchini, M.C., de Leeuw, G., Flossman, A., Chaumerliac, N., Erisman, J.W., 2009. Atmospheric composition change: Ecosystems-Atmosphere interactions. Atmospheric Environment 43, 5193–5267. doi:doi: DOI: 10.1016/j.atmosenv.2009.07.068

Gabrielle, B., Laville, P., Duval, O., Nicoullaud, B., Germon, J.C., Hénault, C., 2006. Process-based modeling of nitrous oxide emissions from wheat-cropped soils at the subregional scale. Global Biogeochemical Cycles 20, GB4018. doi:10.1029/2006GB002686

Gabrielle, B., Mary, B., Roche, R., Smith, P., Gosse, G., 2002a. Simulation of carbon and nitrogen dynamics in arable soils: a comparison of approaches. European Journal of Agronomy 18, 107–120. doi:10.1016/S1161-0301(02)00099-0

Gabrielle, B., Roche, R., Angas, P., Cantero-Martinez, C., Cosentino, L., Mantineo, M., Langensiepen, M., Henault, C., Laville, P., Nicoullaud, B., Gosse, G., 2002b. A priori parameterisation of the CERES soil-crop models and tests against several European data sets. Agronomie 119–132.

Hansen, K., Sørensen, L. L., Hertel, O., Geels, C., Skjøth, C.A., Jensen, B., and Boegh, E.: Ammonia emissions from deciduous forest after leaf fall, Biogeosciences, 10, 4577–4589, doi:10.5194/bg-10-4577-2013, 2013.

Husted, S., Mattsson, M., Schjoerring, J.K., 1996. Ammonia compensation points in two cultivars of Hordeum vulgare L during vegetative and generative growth. Plant Cell and Environment 19, 1299–1306.

Jones, C.A., Kiniry, J.R., 1986. Ceres-N Maize: a simulation model of maize growth and development. Temple, TX.

Langensiepen, M., Hanus, H., Schoop, P., Gräsle, W., 2008. Validating CERES-wheat under North-German environmental conditions. Agricultural Systems 34–47.

Loubet, B., Decuq, C., Personne, E., Massad, R. S., Flechard, C., Fanucci, O., Mascher, N., Gueudet, J.-C., Masson, S., Durand, B., Genermont, S., Fauvel, Y., and Cellier, P.: Investigating the stomatal, cuticular and soil ammonia fluxes over a growing tritical crop under high acidic loads, Biogeosciences, 9, 1537–1552, doi:10.5194/bg-9-1537-2012, 2012

Massad, R.-S., Loubet, B., Tuzet, A., Autret, H., Cellier, P., 2009. Ammonia stomatal compensation point of young oilseed rape leaves during dark/light cycles under various nitrogen nutritions. Agriculture, Ecosystems & Environment 133, 170–182.

Massad, R.S., Loubet, B., Tuzet, A., Cellier, P., 2008. Relationship between ammonia stomatal compensation point and nitrogen metabolism in arable crops: Current status of knowledge and potential modelling approaches. Environmental Pollution 154, 390–403.

Massad, R.-S., Nemitz, E., Sutton, M.A., 2010. Review and parameterisation of bi-directional ammonia exchange between vegetation and the atmosphere. Atmospheric Chemistry and Physics 10, 10359–10386. doi:10.5194/acp-10-10359-2010

Molina, J., Clapp, C., Shaffer, M., Chichester, F., Larson, W., 1983. NCSOIL - a model of nitrogen and carbon transformations in soil: description, calibration, and behavior. Soil Sci. Soc. Am. J. 47, 85–91.

Nemitz, E., Milford, C., Sutton, M.A., 2001. A two-layer canopy compensation point model for describing bi-directional biosphere-atmosphere exchange of ammonia. Quarterly Journal of the Royal Meteorological Society 127, 815–833.

Panagos, P., Van Liedekerke, M., Jones, A., Montanarella, L., 2012. European Soil Data Centre: Response to European policy support and public data requirements. Land Use Policy 29, 329–338. doi:10.1016/j.landusepol.2011.07.003

Rezzoug, W., Gabrielle, B., Suleiman, A., Benabdeli, K., 2008. Application and evaluation of the DSSAT-wheat in the Tiaret region of Algeria. African Journal of Agricultural Research 284–296.

Ritchie, J.T., 1972. Model for predicting evaporation from a row crop with incomplete cover. Water Resources Research 8, 1204–1213. doi:10.1029/WR008i005p01204

Sutton, M.A., Schjoerring, J.K., Wyers, G.P., 1995. Plant-atmosphere exchange of ammonia. Philosophical Transactions of the Royal Society of London. Serie A 261–278.

Wesely, M. L.: Parameterization of surface resistances to gaseous dry deposition in regional-scale numerical models, Atmos. Environ., 23, 1293–1304, 1989.

Xiong, W., Matthews, R., Holman, I., Lin, E., Xu, Y., 2007. Modelling China's potential maize production at regional scale under climate change. Climatic Change 85, 433–451. doi:10.1007/s10584-007-9284-x

**Appendix 1. Summary of the MNS-2010 parameterisation of a two-layer $NH_3$ bi-directional exchange model (Massad et al., 2010).**

<table>
<tr><th colspan="3" rowspan="2"></th><th colspan="2">$\Gamma$</th><th colspan="2">$R_w$</th></tr>
<tr><th>$\Gamma_s$</th><th>$\Gamma_g$</th><th>$R_{wmin}$</th><th>$a$</th></tr>
<tr><td colspan="3">Un-managed</td><td>$\Gamma_s = 246 + (0.0041) \times (N_{in})^{3.56}$</td><td>N/A ($R_g = \infty$)</td><td rowspan="7">$R_w = R_{w(min)} \times e^{a \times (100 - RH)}$<br><br>$R_{w(min)} = 31.5 \times (AR)^{-1}$</td><td rowspan="3">• Forest: 0.0318±0.0179<br><br>• Semi-natural 0.120±0.107</td></tr>
<tr><td rowspan="6">Managed</td><td rowspan="2">Background</td><td>Without vegetation</td><td>N/A ($R_s$ and $R_w = \infty$)</td><td>$\Gamma_g = 500$</td></tr>
<tr><td>With vegetation</td><td>$\Gamma_s = 66.4 + (0.0853) \times (N_{in})^{1.59}$</td><td>N/A ($R_g = \infty$)</td></tr>
<tr><td rowspan="3">Management events</td><td>Mineral fertilisation</td><td rowspan="3">$\Gamma_s = \Gamma_{s(max)} \times e^{(-t/\tau)}$<br><br>$\Gamma_{s(max)} = 12.3 \times N_{app.} + 20.3$<br><br>$\tau$ = 2.88 days</td><td>$\Gamma_g = \Gamma_{g(max)} \times e^{(-t/\tau)}$<br>$\Gamma_{g(max)} = \frac{N_{app} / \theta_s \times M_N \times l_s \times h_m}{10^{-pH}}$<br>$\tau$ = 2.88 days</td><td rowspan="3">• Arable: 0.148±0.113<br><br>• Grassland 0.176±0.126</td></tr>
<tr><td>Organic fertilisation</td><td>$\Gamma_g = \Gamma_{g(max)} \times e^{(-t/\tau)}$<br>$\Gamma_{g(max)} = \frac{TAN_{slurry}}{10^{-pHslurry}}$<br>$\tau$ = 2.88 days</td></tr>
<tr><td>Grazing</td><td>$\Gamma_g = \Gamma_{g(max)} \times e^{(-t/\tau)}$<br>$\Gamma_{g(max)} = 4000$<br>$\tau$ = 2.88 days (after cattle are removed from field)</td></tr>
</table>

$\Gamma$ is unitless; $t$ and $\tau$ are in days; $R_{w(corr)}$ is in s m$^{-1}$;
$N_{in}$ and $N_{app}$ are the total N input to the ecosystem ($N_{app}$+N deposition) and N applied as fertiliser respectively in kg ha$^{-1}$ yr$^{-1}$.

*(Source: Table 8 in Massad et al., 2010, Atmos. Chem. Phys., 10, 10359–10386. www.atmos-chem-phys.net/10/10359/2010/doi:10.5194/acp-10-10359-2010)*